

Efficient Electrical Manipulation of the Magnetization Process in an Epitaxially Controlled $\text{Co}_2\text{FeSi}/\text{BaTiO}_3$ Multiferroic Interface

Shaojie Hu,¹ Shinya Yamada ,^{2,3,4} Po-Chun Chang ,⁵ Wen-Chin Lin,⁵ Kohei Hamaya,^{2,3,4} and Takashi Kimura^{1,3,*}


¹*Department of Physics, Kyushu University, 744 Motoooka, Fukuoka 812-8581, Japan*

²*Department of Systems Innovation, Graduate School of Engineering Science, Osaka University, 1-3 Machikaneyama, Toyonaka, Osaka 560-8531, Japan*

³*Center for Spintronics Research Network, Graduate School of Engineering Science, Osaka University, 1-3 Machikaneyama, Toyonaka, Osaka 560-8531, Japan*

⁴*Spintronics Research Network Division, Institute for Open and Transdisciplinary Research Initiatives, Osaka University, 2-1 Yamadaoka, Suita, Osaka 565-0871, Japan*

⁵*Department of Physics, National Taiwan Normal University, Taipei 11677*

 (Received 24 March 2023; revised 26 May 2023; accepted 4 August 2023; published 14 September 2023)

We investigate the magnetic properties of an epitaxial full-Heusler Co_2FeSi film with an atomically controlled multiferroic interface coupled with a BaTiO_3 substrate. The real-space observation of the magnetic domain structure using a magneto-optical Kerr microscope reveals perfect domain-pattern transfer from the ferroelectric substrate, indicating strong interface magnetoelectric coupling. The unique anisotropic magnetization reversal process was found to be induced by lateral modulation of the magnetic anisotropy constant through the strain-induced magnetoelectric coupling effect. The strong interface coupling yields efficient electrical manipulation of the magnetic property with the appropriate initial ferroelectric domain pattern. Our finding indicates that the interface multiferroic structure based on an epitaxially grown Heusler thin film is a promising approach for efficient electrical manipulation of magnetization.

DOI: [10.1103/PhysRevApplied.20.034029](https://doi.org/10.1103/PhysRevApplied.20.034029)

I. INTRODUCTION

Spintronic devices driven by spin-polarized currents are expected to have attractive properties, such as small cell size, fast switching, and low power consumption [1–3]. Manipulation of the magnetization by electrical means with low power consumption is recognized as a key technique for the development of future spintronic devices. Especially, voltage control of the magnetization has attracted considerable attention owing to its lower power consumption than current-driven manipulation with significant Joule heating [4–9]. Gate-controlled carrier modulation with a moderate voltage is an ideal method [10, 11]. However, it can be applied only in carrier-mediated ferromagnetic semiconductors. Voltage control of antiferromagnetic domain structures has also been demonstrated, but it is limited to magnetic insulators [12].

In ferromagnetic metallic systems, the electric field is known to control the electron filling state in the d orbital, resulting in a change of magnetic anisotropy [5,6,13]. Indeed, various important demonstrations, such as control

of the perpendicular anisotropy, the ferromagnetic resonant property, and the magnetic domain structure, have been reported recently by applying an electrical voltage [14–18]. However, this method can be applied only for an ultrathin ferromagnetic film owing to the extremely short screening length in the metallic system. This significantly reduces the thermal stability of the magnetization state. Since high thermal stability is indispensable in future spintronic devices, this requirement is a serious obstacle in nanoscale spintronic devices. Apart from filling-state control in metallic systems, multiferroic materials with coexisting ferromagnetic (FM) and ferroelectric (FE) domains also have an excellent capability for voltage control of magnetism through strong coupling between electrical and magnetic polarizations [19–25]. However, this kind of attractive property appears only in limited materials, especially at room temperature.

In order to solve the aforementioned issues, multiferroic heterostructures combining ferromagnetic and ferroelectric materials with interface magnetoelectric (ME) coupling, namely interface multiferroic systems, are a promising approach toward the efficient voltage control of magnetism [23,26–30]. The mechanism of voltage-controlled magnetization is mainly due to the strain from the

*t-kimu@phys.kyushu-u.ac.jp

ferroelectric substrate. In addition to the strain effect, other interface interactions such as charge modulation and spin-orbit interaction are known to contribute to the control of the magnetization. The proper combination of these interactions is expected to yield efficient electrical manipulation of the magnetization. However, the details of the magnetoelectric interaction at the FE/FM interface are smeared out by undesired extrinsic effects, such as redox reactions and dislocations at the interface. In order to deepen understanding of the interface magnetoelectric interaction, it is indispensable to form a well-defined FE/FM interface, along with minimizing the extrinsic contribution.

Most of the previous research on the interface magnetoelectric interaction has been carried out by using Fe, CoFe, or other conventional ferromagnetic films grown on BaTiO₃ (BTO) [28,31–36]. On the other hand, a highly spin-polarized FM is theoretically expected to show a significant increment of the interface ME coupling [37]. Recent density-functional theory (DFT) calculations predicted that interface bonding effects play an important role in the anisotropic magnetoresistance and magnetoelectric effects for Co₂FeSi/BaTiO₃ (CFS/BTO) heterostructures [38,39]. Indeed, a large ME coupling constant of $(6.0\text{--}6.3) \times 10^{-6}$ s/m has been reported in the epitaxial *L*₂₁-ordered Co₂FeSi film grown on Pb(Mg_{1/3}Nb_{2/3})O₃-PbTiO₃ (PMN-PT) substrate [40]. Moreover, a giant ME coupling constant of over 1×10^{-5} s/m was found in a Heusler alloy Co₂FeSi with *L*₂₁-ordered structure grown on PMN-PT(011) [41].

However, the underpinnings of elevated ME coupling, as revealed by previous reports, consistently originate from strain [29,42–45]. Concurrently, Yamada *et al.* have developed a fully epitaxial CFS/BTO heterostructure with an atomically controlled interface [46]. This excellent structure provides an ideal platform for the experimental investigation of the contribution from the interface bonding effect as well as for seeking efficient voltage manipulation of magnetic properties. In the present paper, we investigate the magnetization reversal process in an epitaxial CFS/BTO heterostructure and show that a large ME effect can be induced by optimizing the initial (or remanent) ferroelectric domain structure.

II. EXPERIMENTAL

The crystal structure for BTO is known to take a tetragonal crystal system in the temperature range from 278 to 400 K with ferroelectric property and becomes a cubic system with a lattice constant of 0.401 nm above the Curie temperature T_C . Since the lattice constant of CFS is 0.564 nm at room temperature [47,48], which is the diagonal length of the cubic BTO, a fully epitaxial CFS film can be grown on the (001) BTO surface. In the present study, the *L*₂₁-ordered CFS film with a thickness of 30 nm was grown on

the (001) BTO surface at 473 K by using molecular beam epitaxy (MBE) techniques [46].

Figure 1(a) shows a cross-sectional image obtained by scanning transmission electron microscopy (STEM) at the (001) BTO and (001) CFS interface along the [100]_{BTO} and [110]_{CFS} zone axes. From the image, the length of the Ba—Ba bond along [010]_{BTO} is estimated to be 0.391 nm and that for [001]_{BTO} is 0.4037 nm. The bond length between the Co atoms for [110]_{CFS} is 0.391 nm. These results reveal that the in-plane [100]_{BTO} is perfectly acquired along the [110]_{CFS} zone axis, as schematically shown in the inset of Fig. 1(a). From lattice-constant values, we can confirm that CFS is similarly a tetragonal structure consistent with XRD ϕ -scan results [46]. Based on TEM image analysis, it is evident that the termination of the BTO interface is primarily characterized by BaO. It is worth noting that there are Ba vacancies around the interface. The gradual contrast change near the interface may be attributed to oxidation of the Co atoms. Therefore, such complex interface conditions may blur the predicted bonding effect in theory [39].

The lateral size for the present CFS/BTO multiferroic sample is 5 mm square and the thickness of the BTO substrate is 500 μm . After growing the CFS film, the crystal structure for the BTO becomes a tetragonal system during the sample cooling process across the Curie temperature. Here, the elongated direction in the tetragonal system can be normal to the plane (*c* domain) or in-plane (*a* domain), depending on the direction of the electric polarization. However, in order to reduce the internal stress of the BTO with the tetragonal system, a periodic domain structure consisting of *a* – *c* strip domains is formed at the surface of the BTO.

From the polarized optical microscope image shown in Fig. 1(b), the BTO substrate for the present study is found to consist of three kinds of ferroelectric domain patterns composed of an *a*₁ – *c* strip domain along the [100]_{BTO} direction, an *a*₂ – *c* strip domain along the [010]_{BTO} direction, and uniform *c* domains, in the present sample. The typical lateral size of the periodic domains is approximately 10 μm . The three domain regions are not uniformly distributed on the substrate from the optical microscope image. Their distributions strongly depend on the substrate and electric field treatment history. The 200-nm-thick Cu was deposited on the bottom of the opposite side of the surface as a back-gate electrode for applying an electric field.

III. RESULTS AND DISCUSSION

In order to evaluate the magnetization characteristics of the epitaxial CFS grown on the BTO, we have measured the magnetic hysteresis loop (*M*-*H* loop) by using a vibrating sample magnetometer (VSM). Figures 2(a) and 2(b) show the magnetic hysteresis loops of the CFS under an

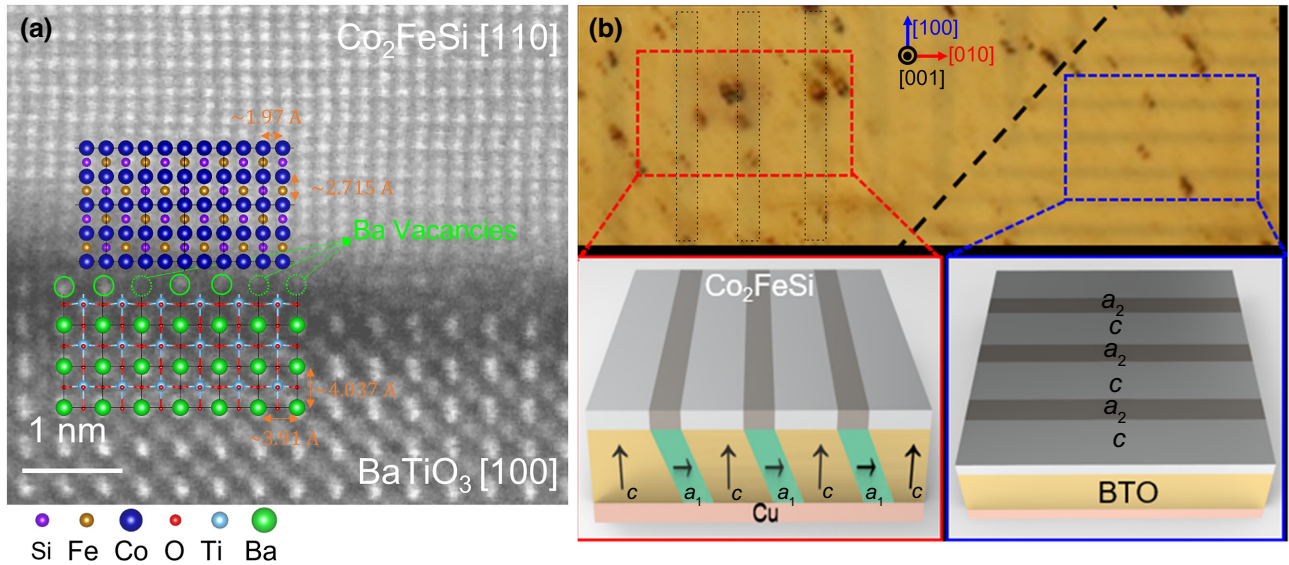


FIG. 1. (a) Cross-sectional STEM image of an atomically controlled epitaxial $\text{Co}_2\text{FeSi}/\text{BaTiO}_3$ interface together with a schematic illustration of the atomic geometry. (b) Polarized-light microscope image of the $\text{Co}_2\text{FeSi}/\text{BaTiO}_3$ sample for ferroelectric domain observation. The dark strips correspond to a_1 domains elongated along the $[010]_{\text{BTO}}$ direction or a_2 domains elongated along the $[100]_{\text{BTO}}$ direction, while the light strips are the c domain elongated along the $[001]_{\text{BTO}}$ direction.

in-plane magnetic field along the $[010]_{\text{BTO}}$ and $[100]_{\text{BTO}}$ directions, respectively. Enlarged plots at low magnetic field are shown in Figs. 2(c) and 2(d), respectively. In Fig. 2(c), a magnetization reversal process accompanied by two irreversible switchings has been clearly observed. A similar two-step magnetization process has been reported in ferromagnetic systems with a biaxial magnetocrystalline anisotropy due to the fourfold symmetry [49] and the micro-sized magnetic wires with the crystal magnetic anisotropy [50].

Since the crystal structure of CFS is a body-centered cubic lattice with fourfold symmetry [51], the observed two-step switching process seems to be related to the biaxial magnetic anisotropy. However, as shown in Fig. 2(b), this two-step signature disappeared after a 90° rotation. This is inconsistent with the biaxial anisotropy originating from fourfold symmetry. Therefore, the biaxial crystal anisotropy cannot fully explain the observation of the magnetization process. Lahtinen *et al.* also reported a two-step switching behavior in a Fe/BTO multiferroic system with $a-c$ strip domains because of laterally modulated strain with magnetostatic interaction [28]. In the present case, CFS grown on the c domain of BTO does not feel any stress from the BTO because of the perfect matching of the lattice parameters. This may produce the unique modulation of the magnetic anisotropy in the CFS magnetization coupled with the ferroelectric $a-c$ strip domains. In order to provide the proper description of the magnetization process of CFS, it is essential to investigate the magnetoelectric coupling effects more clearly.

To obtain further information related to the ME coupling effect in the present system, we should consider the magnetization on the different ferroelectric domain patterns individually. The real-space observation of the magnetization process was performed by using magneto-optical Kerr

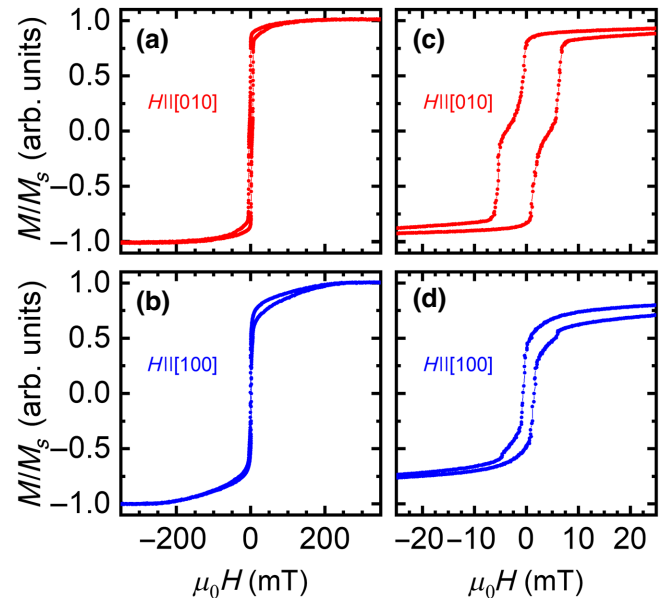


FIG. 2. (a) The M - H loop of epitaxial CFS/BTO under a magnetic field along the $[010]_{\text{BTO}}$ direction and (b) that along the $[100]_{\text{BTO}}$ direction. The magnetic moment has been measured by VSM. (c) Enlarged plot of panel (a) at low magnetic field and (d) similar enlarged plot of panel (b).

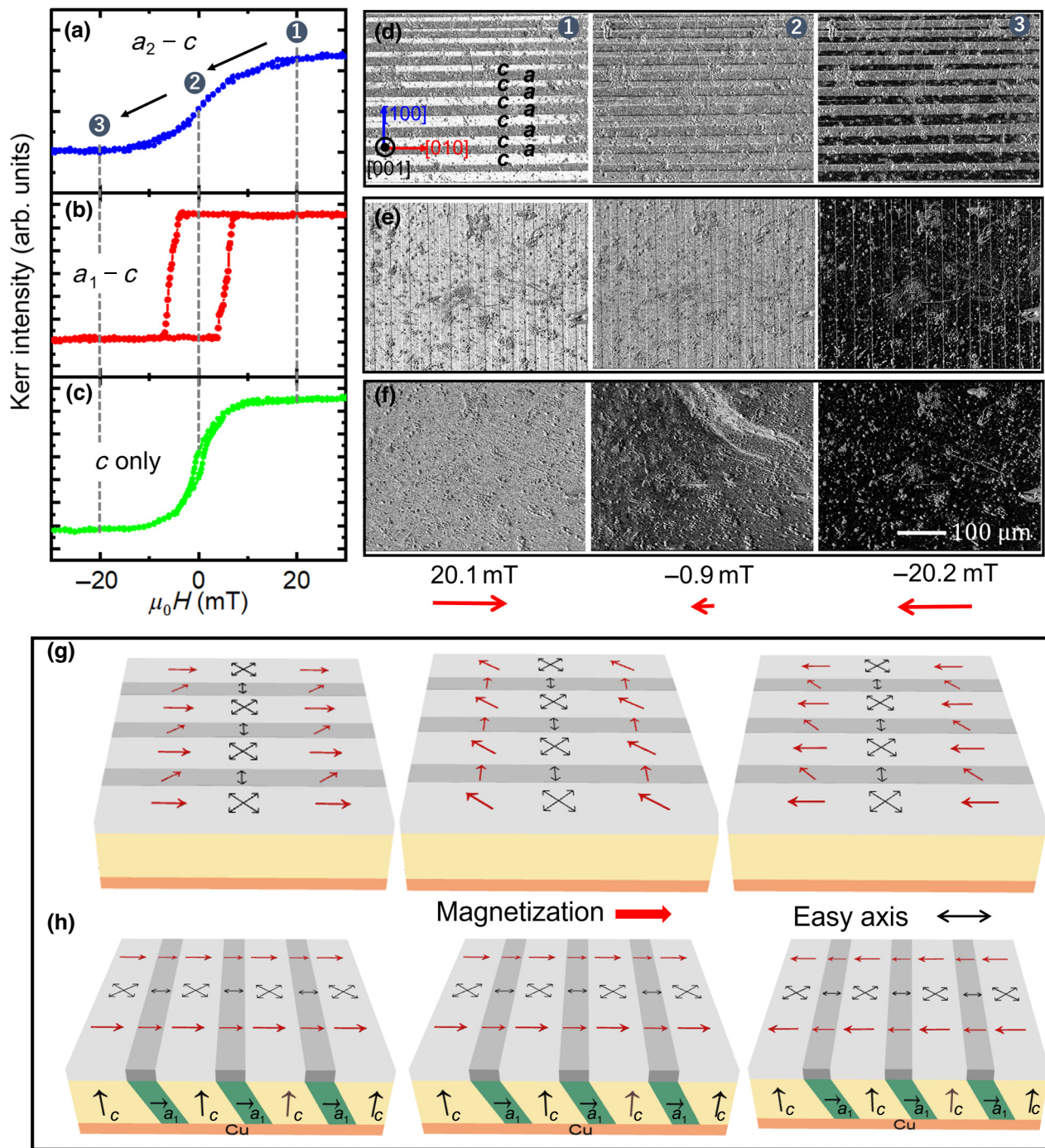


FIG. 3. (a) MOKE M - H loop in the $a_2 - c$ strip domain, (b) that in the $a_1 - c$ strip domain, and (c) that in the uniform c domain for the CFS/BTO sample. (d)–(f) The magnetic domain patterns observed by Kerr microscopy using the focused laser beam; panels (d)–(f) correspond to the areas for the $a_2 - c$ strip, the $a_1 - c$ strip, and uniform c domains, respectively. (g) Schematic of the expected magnetization process for the CFS films coupled with the $a_2 - c$ domain and (h) that for the $a_1 - c$ domain.

effect (MOKE) microscopy with a focused laser beam. From the MOKE image, the magnetic domain of the CFS film was found to be divided into three different patterns consisting of two types of strip domains and a uniform domain. Here, the two types of strip domains are vertically

aligned and horizontally aligned alternate patterns. These results can be well understood by the pattern transfer from the ferroelectric into the ferromagnetic domains, indicating a strong ME coupling between the CFS and the BTO.

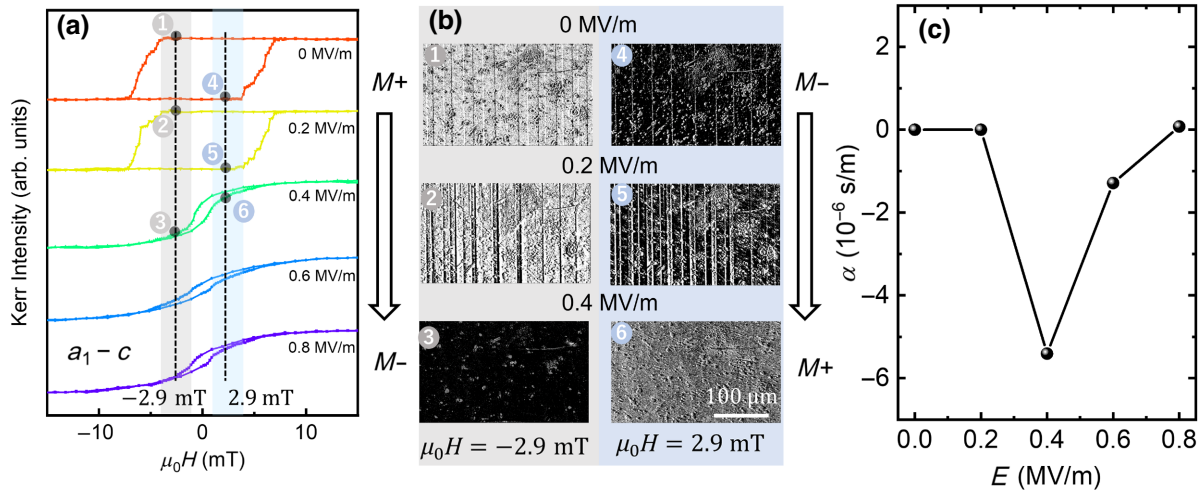


FIG. 4. (a) MOKE $M-H$ loops in the ferroelectric $a_1 - c$ strip domain under the application of various electric fields. (b) Ferromagnetic domain patterns during the magnetization reversal process under various magnetic fields. The imaging patterns correspond to the related positions marked as 1–6 in the hysteresis curves. (c) The electric field dependence of the magnetoelectric coupling coefficient α at zero magnetic field.

Figures 3(a)–3(c) show the MOKE $M-H$ curves together with MOKE images for the three different patterns [Fig. 3(d)–3(f)]. Here, the magnetic field is applied along the horizontal direction, which is parallel to the $[010]_{\text{BTO}}$ direction. First, we focus on the magnetization process for the vertically aligned strip domain, which corresponds to the ferroelectric $a_2 - c$ strip domain. In Fig. 3(a), the magnetization shows a broad linear change with a rapid change in slope below 10 mT and a small increase above 10 mT. As can be seen in the MOKE image, a clear magnetic strip domain is still observed above $H = 20$ mT, indicating that the part of the magnetization coupled with the a_2 ferroelectric domain does not align with the magnetic field while that coupled with the c domain fully aligned with the magnetic field at 10 mT.

For the magnetization coupled with the a_2 domain, the magnetic anisotropy is induced by the strain from the BTO. Since the BTO domain is elongated along the electric polarization, the magnetic anisotropy is induced by the inverse magnetostriction effect in the CFS. From the experimental fact that the direction normal to the expanded direction, which is parallel to the $[010]_{\text{BTO}}$ direction, is a magnetically hard axis for CFS, the magnetostriction coefficient for CFS is found to be positive. For the magnetization coupled with the c domain, since there is no stress from the BTO, the observed magnetically hard signature in the low magnetic field originates from the crystal nature of the CFS. This is consistent with the cubic crystal structure of the epitaxial CFS. Thus, the MOKE $M-H$ loop for the magnetization coupled with the $a_2 - c$ strip domain can be understood by the combination of the two hard-axis magnetization processes with different magnetic anisotropies as schematically shown in Fig. 3(g).

On the other hand, in the $a_1 - c$ domain where the magnetic field is normal to the strip, we observed a sharp rectangular $M-H$ loop with a single switching process. From the viewpoint of magnetostriction, since the $[010]_{\text{BTO}}$ direction is an easy axis for the CFS magnetization coupled with the a_1 domain, the rectangular hysteresis loop can be understood by the inverse magnetostriction effect. For the magnetization coupled with the c domain, the $[010]_{\text{BTO}}$ direction is a magnetically hard axis from the viewpoint of magnetocrystalline anisotropy. However, as can be seen in Fig. 3(e), we did not observe a strip magnetic domain pattern in the MOKE image during the magnetization reversal process. This is because the magnetocrystalline anisotropy is smaller than the exchange energy and the magnetostatic energy at the boundary. Therefore, the magnetization coupled with the c domain behaves similarly to the magnetization coupled with the a_1 domain, leading to the a sharp rectangular $M-H$ loop, as schematically shown in Fig. 3(h).

Thus, the difference in the magnetic anisotropy between the vertical and horizontal strip domains produces a unique angular dependence of the $M-H$ loop. For magnetization coupled with the uniform ferroelectric c domain, the $M-H$ loop exhibits a standard hard-axis character with biaxial magnetic anisotropy. We also emphasize that the shapes of the $M-H$ loops for the $a_1 - c$ and $a_2 - c$ strip domains are interchanged by a 90° rotation of the external magnetic field. Thus, the magnetization processes coupled with various ferroelectric domains can be fully understood by a combination of strain-induced magnetic anisotropy and magnetocrystalline anisotropy.

Based on these results, we are able to provide a consistent description of the $M-H$ loops measured by the VSM

for the whole region of the sample shown in Fig. 2. The total M - H loop for the whole region can be understood as the sum of three different magnetization processes coupled with the different ferroelectric domain patterns. The two-step switching process shown in Fig. 2(c) can be understood by two switching processes originating from the irreversible rotation of the magnetization coupled with the uniform c domain and the easy-axis magnetization switching coupled with the $a_2 - c$ domain. The large saturation field observed in Fig. 2 is caused by the strain-induced magnetic anisotropy in the magnetization coupled with the $a_1 - c$ domain. Here, the magnetic anisotropy constant for the $a_1 - c$ domain is $K_S = 0.12$ MJ/m³, while that for the uniform c domain, where there is biaxial anisotropy originating from the fourfold crystal structure, is $K_{CFS} = 0.005$ MJ/m³. On the a domain of BTO, the long axis is in the plane of CFS. Hence, a uniaxial magnetic anisotropy can be generated. The anisotropy constant for the $a_1 - c$ strip domain is over one order higher than that for the c domain. This significant difference in anisotropy constants indicates that the uniaxial anisotropy constant of a domain can be recognized as that of the $a_1 - c$ strip domain. If a high out-of-plane electric field is applied to the a domain, a strain-induced ME effect on the CFS/BTO system will drastically affect the anisotropic magnetic constant of CFS when the a domain is changed to the c domain.

We next focus on the effect of the electric field on the magnetization process. Since a sufficiently large electric field using the Cu back-gate electrode induces the ferroelectric domain change from the $a_1 - c$ strip domain to the uniform c domain, we expect a significant change of the magnetization property by the application of the electric field. Figure 4 shows the M - H loops under various electric fields. With increasing electric field, the shape of the hysteresis loop changes from a rectangle to a broad change. Here, the normalized remanent magnetization M_r/M_s changes from 1.0 at $E = 0$ MV/m to 0.32 at $E = 0.4$ MV/m, which is the coercive electric field for the BTO. The electric field dependence of the magnetoelectric coupling coefficient α , which is estimated from the relation $\mu_0 dM_r/dE$, is shown in Fig. 4(c). The coefficient α exceeds -5.8×10^{-6} s/m, which is a relatively large value reported so far [29,30,40]. Such a large α indicates that the mechanism for the modulation of the magnetic anisotropy in the present system is dominated by the strain nature. Thus, optimizing the original ferroelectric domain structure facilitates an efficient electric modulation of magnetization by strain.

IV. CONCLUSION

We have investigated the magnetoelectric effect in an epitaxial Co₂FeSi/BaTiO₃ multiferroic interface. We confirmed that the ferroelectric domain patterns of the BTO surface perfectly transfer to the ferromagnetic domain

structures. The magnetization process is found to show a unique angular dependence due to the strain-induced magnetic anisotropy with the magnetostatic interaction. By optimizing the ferroelectric domain pattern coupled with the ferromagnetic film, we are able to obtain a large magnetoelectric coupling coefficient, assuring strong interface magnetoelectric coupling. These results indicate that the atomically controlled epitaxial ferromagnetic/ferroelectric interface is able to induce multiferroic properties efficiently.

The data that support the findings of this study are available from the corresponding author upon reasonable request.

ACKNOWLEDGMENTS

We thank Prof. Y. Gohda for his valuable comments. This work is partially supported by the JST CREST (JPMJCR18J1), JSPS Program 351 of Grant-in-Aid for Scientific Research (S)(21H05021, 22H05000, 19H05616), Grant-in-Aid for Challenging Research (Exploratory) (20K21002) and JST SICORP Program (22480474).

The authors declare that there is no conflict of interest.

-
- [1] S. A. Wolf, D. D. Awschalom, R. A. Buhrman, J. M. Daughton, von S. von Molnár, M. L. Roukes, A. Yu Chtchelkanova, and D. M. Treger, Spintronics: A spin-based electronics vision for the future, *Science* **294**, 1488 (2001).
 - [2] Igor Žutić, Jaroslav Fabian, and S. Das Sarma, Spintronics: Fundamentals and applications, *Rev. Mod. Phys.* **76**, 323 (2004).
 - [3] Samuel D. Bader and S. S. P. Parkin, Spintronics, *Annu. Rev. Condens. Matter Phys.* **1**, 71 (2010).
 - [4] H. Ohno, a. D. Chiba, a. F. Matsukura, T. Omiya, E. Abe, T. Dietl, Y. Ohno, and K. Ohtani, Electric-field control of ferromagnetism, *Nature* **408**, 944 (2000).
 - [5] Martin Weisheit, Sebastian FÄhler, Alain Marty, Yves Souche, Christiane Poinsonon, and Dominique Givord, Electric field-induced modification of magnetism in thin-film ferromagnets, *Science* **315**, 349 (2007).
 - [6] T. Maruyama, Y. Shiota, T. Nozaki, K. Ohta, N. Toda, M. Mizuguchi, A. A. Tulapurkar, T. Shinjo, M. Shiraishi, and S. Mizukami, *et al.*, Large voltage-induced magnetic anisotropy change in a few atomic layers of iron, *Nat. Nanotechnol.* **4**, 158 (2009).
 - [7] Jian Zhu, J. A. Katine, Graham E. Rowlands, Yu-Jin Chen, Zheng Duan, Juan G. Alzate, Pramey Upadhyaya, Juer-gen Langer, Pedram Khalili Amiri, and Kang L. Wang, *et al.*, Voltage-Induced Ferromagnetic Resonance in Magnetic Tunnel Junctions, *Phys. Rev. Lett.* **108**, 197203 (2012).
 - [8] Fumihiko Matsukura, Yoshinori Tokura, and Hideo Ohno, Control of magnetism by electric fields, *Nat. Nanotechnol.* **10**, 209 (2015).
 - [9] Kang Wang, Shaojie Hu, Fupeng Gao, Miaoxin Wang, and Dawei Wang, Dual function spin-wave logic gates based on

- electric field control magnetic anisotropy boundary, *Appl. Phys. Lett.* **120**, 142405 (2022).
- [10] Y. Ohno, D. K. Young, B. al Beschoten, Fumihiko Matsukura, Hideo Ohno, and D. D. Awschalom, Electrical spin injection in a ferromagnetic semiconductor heterostructure, *Nature* **402**, 790 (1999).
- [11] D. Chiba, M. Yamanouchi, F. Matsukura, and H. Ohno, Electrical manipulation of magnetization reversal in a ferromagnetic semiconductor, *Science* **301**, 943 (2003).
- [12] Yu Shiratsuchi, Kentaro Toyoki, and Ryoichi Nakatani, Magnetolectric control of antiferromagnetic domain state in Cr₂O₃ thin film, *J. Phys.: Condens. Matter* **33**, 243001 (2021).
- [13] Jun Okabayashi, Yoshio Miura, and Tomoyasu Taniyama, Strain-induced reversible manipulation of orbital magnetic moments in Ni/Cu multilayers on ferroelectric BaTiO₃, *npj Quantum Mater.* **4**, 21 (2019).
- [14] F. Zavaliche, H. Zheng, L. Mohaddes-Ardabili, S. Y. Yang, Q. Zhan, P. Shafer, E. Reilly, R. Chopdekar, Y. Jia, and P. Wright, *et al.*, Electric field-induced magnetization switching in epitaxial columnar nanostructures, *Nano Lett.* **5**, 1793 (2005).
- [15] Vladimir Laukhin, Vassil Skumryev, X. Martí, D. Hrabovsky, F. Sánchez, M. V. García-Cuenca, C. Ferrater, M. Varela, U. Lüders, and Jean-François Bobo, *et al.*, Electric-Field Control of Exchange Bias in Multiferroic Epitaxial Heterostructures, *Phys. Rev. Lett.* **97**, 227201 (2006).
- [16] Ying-Hao Chu, Lane W. Martin, Mikel B. Holcomb, Martin Gajek, Shu-Jen Han, Qing He Nina Balke, Chan-Ho Yang, and Donkoun Lee, *et al.*, Electric-field control of local ferromagnetism using a magnetoelectric multiferroic, *Nat. Mater.* **7**, 478 (2008).
- [17] Ji Young Jo, Sang Mo Yang, T. H. Kim, Ho Nyung Lee, J.-G. Yoon, S. Park, Y. Jo, M. H. Jung, and Tae Won Noh, Nonlinear Dynamics of Domain-Wall Propagation in Epitaxial Ferroelectric Thin Films, *Phys. Rev. Lett.* **102**, 045701 (2009).
- [18] Yuxin Cheng, Shishun Zhao, Ziyao Zhou, and Ming Liu, Recent development of E-field control of interfacial magnetism in multiferroic heterostructures, *Nano Res.* **16**, 5983 (2023).
- [19] Tsuyoshi Kimura, T. Goto, H. Shintani, K. Ishizaka, T.-h. Arima, and Y. Tokura, Magnetic control of ferroelectric polarization, *Nature* **426**, 55 (2003).
- [20] Ramaroorthy Ramesh and Nicola A. Spaldin, Multiferroics: Progress and prospects in thin films, *Nat. Mater.* **6**, 21 (2007).
- [21] H. F. Tian, T. L. Qu, L. B. Luo, J. J. Yang, S. M. Guo, H. Y. Zhang, Y. G. Zhao, and J. Q. Li, Strain induced magnetoelectric coupling between magnetite and BaTiO₃, *Appl. Phys. Lett.* **92**, 063507 (2008).
- [22] Ming Liu, Ogheneyunume Obi, Jing Lou, Yajie Chen, Zhuhua Cai, Stephen Stoute, Mary Espanol, Magnum Lew, Xiaodan Situ, and Kate S. Ziemer, *et al.*, Giant electric field tuning of magnetic properties in multiferroic ferrite/ferroelectric heterostructures, *Adv. Funct. Mater.* **19**, 1826 (2009).
- [23] Y. Shirahata, T. Nozaki, G. Venkataiah, H. Taniguchi, M. Itoh, and T. Taniyama, Switching of the symmetry of magnetic anisotropy in Fe/BaTiO₃ heterostructures, *Appl. Phys. Lett.* **99**, 022501 (2011).
- [24] Morgan Trassin, J. D. Clarkson, Samuel R. Bowden, Jian Liu, J. T. Heron, R. J. Paull, E. Arenholz, D. T. Pierce, and J. Unguris, Interfacial coupling in multiferroic/ferromagnet heterostructures, *Phys. Rev. B* **87**, 134426 (2013).
- [25] M. Endo, S. Kanai, S. Ikeda, F. Matsukura, and H. Ohno, Electric-field effects on thickness dependent magnetic anisotropy of sputtered MgO/Co₄₀Fe₄₀B₂₀/Ta structures, *Appl. Phys. Lett.* **96**, 212503 (2010).
- [26] Chun-Gang Duan, Sitaram S. Jaswal, and Evgeny Y. Tsymbal, Predicted Magnetolectric Effect in Fe/BaTiO₃ Multilayers: Ferroelectric Control of Magnetism, *Phys. Rev. Lett.* **97**, 047201 (2006).
- [27] Laura Bocher, Alexandre Gloter, Arnaud Crassous, Vincent Garcia, Katia March, Alberto Zobelli, Sergio Valencia, Shaïma Enouz-Vedrenne, Xavier Moya, and Neil D. Marthur, *et al.*, Atomic and electronic structure of the BaTiO₃/Fe interface in multiferroic tunnel junctions, *Nano Lett.* **12**, 376 (2012).
- [28] Tuomas H. E. Lahtinen, Yasuhiro Shirahata, Lide Yao, Kevin J. A. Franke, Gorige Venkataiah, Tomoyasu Taniyama, and Sebastiaan van Dijken, Alternating domains with uniaxial and biaxial magnetic anisotropy in epitaxial Fe films on BaTiO₃, *Appl. Phys. Lett.* **101**, 262405 (2012).
- [29] Cheng Song, Bin Cui, Fan Li, Xiangjun Zhou, and Feng Pan, Recent progress in voltage control of magnetism: Materials, mechanisms, and performance, *Prog. Mater. Sci.* **87**, 33 (2017).
- [30] J. Wang, D. Pesquera, R. Mansell, S. Van Dijken, R. P. Cowburn, M. Ghidini, and N. D. Mathur, Giant non-volatile magnetoelectric effects via growth anisotropy in Co₄₀Fe₄₀B₂₀ films on PMN-PT substrates, *Appl. Phys. Lett.* **114**, 092401 (2019).
- [31] Sarbeswar Sahoo, Srinivas Polisetty, Chun-Gang Duan, Sitaram S. Jaswal, Evgeny Y. Tsymbal, and Christian Binek, Ferroelectric control of magnetism in BaTiO₃/Fe heterostructures via interface strain coupling, *Phys. Rev. B* **76**, 092108 (2007).
- [32] G. Venkataiah, Y. Shirahata, M. Itoh, and T. Taniyama, Manipulation of magnetic coercivity of Fe film in Fe/BaTiO₃ heterostructure by electric field, *Appl. Phys. Lett.* **99**, 102506 (2011).
- [33] G. Venkataiah, Y. Shirahata, I. Suzuki, M. Itoh, and T. Taniyama, Strain-induced reversible and irreversible magnetization switching in Fe/BaTiO₃ heterostructures, *J. Appl. Phys.* **111**, 033921 (2012).
- [34] G. Venkataiah, E. Wada, H. Taniguchi, M. Itoh, and T. Taniyama, Electric-voltage control of magnetism in Fe/BaTiO₃ heterostructured multiferroics, *J. Appl. Phys.* **113**, 17C701 (2013).
- [35] Venkataiah Gorige, Anupama Swain, Katsuyoshi Komatsu, Mitsuru Itoh, and Tomoyasu Taniyama, Magnetization reversal in Fe/BaTiO₃ (110) heterostructured multiferroics, *Phys. Status Solidi (RRL)–Rap. Res. Lett.* **11**, 1700294 (2017).
- [36] Stefano Brivio, Daniela Petti, Riccardo Bertacco, and J. C. Cezar, Electric field control of magnetic anisotropies and magnetic coercivity in Fe/BaTiO₃ (001) heterostructures, *Appl. Phys. Lett.* **98**, 092505 (2011).

- [37] Chun-Gang Duan, Julian P. Velez, Renat F. Sabirianov, Ziqiang Zhu, Junhao Chu, Sitaram S. Jaswal, and Evgeny Y. Tsybal, Surface Magnetoelectric Effect in Ferromagnetic Metal Films, *Phys. Rev. Lett.* **101**, 137201 (2008).
- [38] Jinfeng Chen, Chensheng Lin, Yi Yang, and Lei Hu Wendan Cheng, Ab initio study of the magnetoelectric effect and critical thickness for ferroelectricity in $\text{Co}_2\text{FeSi}/\text{BaTiO}_3$ multiferroic tunnel junctions, *Modell. Simul. Mater. Sci. Eng.* **22**, 015008 (2013).
- [39] Shunsuke Tsuna, Rafael Costa-Amaral, and Yoshihiro Gohda, Origin of anisotropic magnetoresistance tunable with electric field in $\text{Co}_2\text{FeSi}/\text{BaTiO}_3$ multiferroic interfaces, *J. Appl. Phys.* **132**, 234101 (2022).
- [40] T. Usami, S. Fujii, S. Yamada, Y. Shiratsuchi, R. Nakatani, and K. Hamaya, Giant magnetoelectric effect in an $L2_1$ -ordered $\text{Co}_2\text{FeSi}/\text{Pb}(\text{Mg}_{1/3}\text{Nb}_{2/3})\text{O}_3$ - PbTiO_3 multiferroic heterostructure, *Appl. Phys. Lett.* **118**, 142402 (2021).
- [41] Shumpei Fujii, Takamasa Usami, Yu Shiratsuchi, Adam M. Kerrigan, Amran Mahfudh Yatmeidhy, Shinya Yamada, Takeshi Kanashima, Ryoichi Nakatani, Vlado K. Lazarov, and Tamio Oguchi, *et al.*, Giant converse magnetoelectric effect in a multiferroic heterostructure with polycrystalline Co_2FeSi , *NPG Asia Mater.* **14**, 43 (2022).
- [42] Jia-Mian Hu, Chun-Gang Duan, Ce-Wen Nan, and Long-Qing Chen, Understanding and designing magnetoelectric heterostructures guided by computation: Progresses, remaining questions, and perspectives, *npj Comput. Mater.* **3**, 18 (2017).
- [43] M. Ghidini, R. Mansell, F. Maccherozzi, X. Moya, L. C. Phillips, W. Yan, D. Pesquera, C. H. W. Barnes, R. P. Cowburn, and J.-M. Hu, *et al.*, Shear-strain-mediated magnetoelectric effects revealed by imaging, *Nat. Mater.* **18**, 840 (2019).
- [44] P. B. Meisenheimer, R. A. Steinhardt, S. H. Sung, L. D. Williams, S. Zhuang, M. E. Nowakowski, S. Novakov, M. M. Torunbalci, Bhagwati Prasad, and C. J. Zollner, *et al.*, Engineering new limits to magnetostriction through metastability in iron-gallium alloys, *Nat. Commun.* **12**, 2757 (2021).
- [45] Adrian Begue and Miguel Ciria, Strain-mediated giant magnetoelectric coupling in a crystalline multiferroic heterostructure, *ACS Appl. Mater. Interfaces* **13**, 6778 (2021).
- [46] S. Yamada, Y. Teramoto, D. Matsumi, D. Kepaptsoglou, I. Azaceta, T. Murata, K. Kudo, V. K. Lazarov, T. Taniyama, and K. Hamaya, Electric field tunable anisotropic magnetoresistance effect in an epitaxial $\text{Co}_2\text{FeSi}/\text{BaTiO}_3$ interfacial multiferroic system, *Phys. Rev. Mater.* **5**, 014412 (2021).
- [47] Sabine Wurmehl, Gerhard H. Fecher, Hem C. Kandpal, Vadim Ksenofontov, Claudia Felser, Hong-Ji Lin, and Jander Morais, Geometric, electronic, and magnetic structure of Co_2FeSi : Curie temperature and magnetic moment measurements and calculations, *Phys. Rev. B* **72**, 184434 (2005).
- [48] Benjamin Balke, Gerhard H. Fecher, Hem C. Kandpal, Claudia Felser, Keisuke Kobayashi, Eiji Ikenaga, Jung-Jin Kim, and Shigenori Ueda, Properties of the quaternary half-metal-type Heusler alloy $\text{Co}_2\text{Mn}_{1-x}\text{Fe}_x\text{Si}$, *Phys. Rev. B* **74**, 104405 (2006).
- [49] C. Daboo, R. J. Hicken, E. Gu, M. Gester, S. J. Gray, D. E. P. Eley, E. Ahmad, J. A. C. Bland, R. Ploessl, and J. N. Chapman, Anisotropy and orientational dependence of magnetization reversal processes in epitaxial ferromagnetic thin films, *Phys. Rev. B* **51**, 15964 (1995).
- [50] U. Ebels, A. O. Adeyeye, M. Gester, R. P. Cowburn, C. Daboo, and J. A. C. Bland, Anisotropic domain evolution in epitaxial Fe/GaAs (001) wires, *Phys. Rev. B* **56**, 5443 (1997).
- [51] Weihua Zhu, Yu Zhang, Zhihao Ji, Zhong Shi, Q. Y. Jin, and Zongzhi Zhang, Thickness dependent structural ordering and magnetic properties of Co_2FeSi films with or without a Cr buffer layer, *J. Phys. D: Appl. Phys.* **52**, 355005 (2019).